Send Orders for Reprints to reprints@benthamscience.ae

The Open Automation and Control Systems Journal, **2015,** *7,* **21-30**

Modeling and Optimization Control for Aircraft AC Generator Brushless Excitation System Based on Improved Adaptive PSO

Ruofa Cheng*, Wenlong Zhao, Hongfeng Deng and Xiaozhou Jiang

School of Information Engineering, Nanchang Hangkong University, Nanchang, 330063, China

Abstract: The brushless excitation system of aircraft AC generator is a strong coupled and nonlinearity dynamic system which is often being subjected to disturbances. Therefore, the conventional PID controller is unable to meet the brushless excitation system control requirements of More Electric Aircraft (MEA) or All Electric Aircraft (AEA). A new brushless excitation compound control controller (RBFPID) is proposed in this paper based on radical basis function (RBF) neural networks and the conventional PID control. Because the new brushless excitation compound controller (RBFPID) has a number of mutually coupled parameters that needs to be set, the improved adaptive particle swarm optimization (APSO) algorithm is used to optimize mutually coupled PID parameters Kp, Ki, Kd and RBF parameters η, α, m, n on line. In order to validate performances of the new brushless excitation compound controller based on multi-parameter optimization by the improved APSO, the simulation model of the aircraft brushless excitation system is implemented in MATLAB/SIMULINK according to differential equations of each component of brushless excitation system. The simulation results show that the optimized adaptive compound excitation controller (APSORBFPID) exhibits quick response speed, short adjustment time and high steady state accuracy.

Keywords: Aircraft generator, brushless excitation system, modeling and optimiztion control, PSO, RBF neural network.

1. INTRODUCTION

With the rapid development of More Electric Aircraft (MEA) and All Electric Aircraft (AEA) technology, the structure and control function of aircraft electrical system has become much more complex. The brushless excitation control system is a critical component of the aircraft electric power system, and its performance directly affects the whole aircraft power system stability and reliability. Thus it is very important and necessary to design a stable and reliable excitation controller for aircraft AC generator.

The traditional Proportional Integral Derivative (PID) controller has been widely applied to the excitation control of synchronous generator [1, 2], because it has the advantages of simple structure, good robustness, easy to implement, no steady state error. However, it is hard to build the accurate mathematical model for complex MEA/AEA excitation control system due to the challenge of nonlinearity, multi-variable, strong coupling and time-varying. Therefore, it is difficult to obtain satisfactory control effectiveness in complex MEA/AEA power system by using the traditional PID control strategy based on mathematical model. In recent years, many scholars have studied some new excitation control strategies and parameter optimization for complex power system, such as fuzzy control [3], genetic algorithm (GA) [4], particle swarm optimization (PSO) [5]. But fuzzy control effectiveness depends largely on membership function and fuzzy rules; Genetic algorithm or particle swarm optimization is prone to local optimum, premature convergence.

Neural network technology has made great progress in recent years and has been widely applied in control field, especially radical basis function (RBF) [6, 7], which is a neural network based on local learning. RBF neural network has many attractive characters such as adaptability, nonlinear approximation ability, easy to realize and so on. It is more suitable for nonlinear real-time complex control system. RBF and PID compound controllers have the characteristics of high precision, good real-time and robustness, but too many parameters need to be adjusted in control process. It is difficult to tune because of coupling among the parameters. If improper selection of parameters will obtain bad control effectiveness, and even cause the system to be unstable. The literature [8] demonstrated that fixed gain PI controller can achieve locally finite stability when the system has RBF estimation bias or random disturbance. The literature [9] uses IPSO for PID controller optimal design. The GA is used for PID controller optimization in literature [10]. The literature [11] has put forward a hierarchical learning rate factor, which is introduced into RBF learning. The above literatures obtained some good results, but they did not consider the coupling and coordinative optimization of different control parameters among RBF and PID. In order to overcoming the afore mentioned shortcomings, an innovative multi-parameter coordinative optimization scheme for PID and RBF compound excitation control is proposed in this paper, which is based on adaptive particle swarm optimization algorithm.

This paper is organized as follows. Brushless excitation system model for aircraft AC generator is established in Sec-

*Address corresponding to this author at School of Information Engineering, Nanchang Hangkong University, Nanchang, Jiangxi, 330063, China; Tel: 0867983953473; E-mail: cjbyong@126.com

1874-4443/15

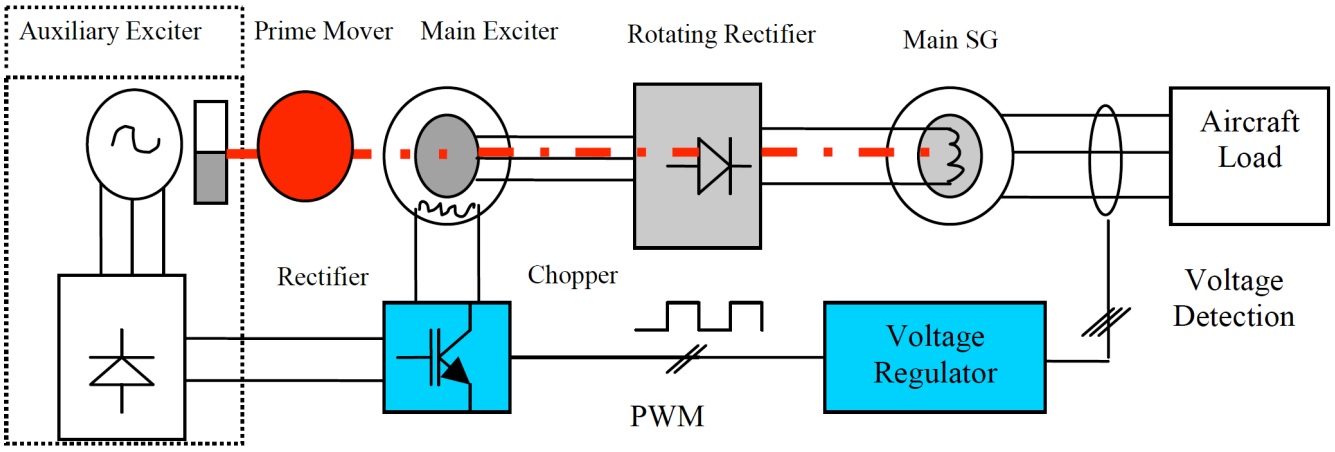

Fig. (1). PID and RBF adaptive controller based on PSO.

tion 2. In Section 3, the new RBF and PID compound excitation controller is designed based on APSO multi-parameter optimization. Then simulation experiment and result are demonstrated in Section 4. Finally, the paper is concluded in Section 5.

2. EXCITATION SYSTEMN MODEL

2.1. Aircraft Generator Brushless Excitation System

At present, three-stage AC synchronous generator brushless excitation system is used in large and medium-sized aircraft, which includes the auxiliary exciter, main AC exciter and main generator [12]. The main generator is a rotating magnetic pole synchronous generator. The main generator field current is provided by the output of the rotating rectifier, which is set in the same rotating spindle with rotating armature of the AC exciter. The auxiliary exciter is a permanent magnet synchronous motor (PMSM) that is a rotating magnetic pole synchronous generator. The structure of three-stage aircraft AC generator brushless excitation system is shown in Fig. (**1**). The main exciter and excitation controller are provided with DC power supply, which is the rectification output voltage of permanent magnet synchronous generator. The excitation controller adjusts main AC exciter excitation current with some control algorithm. Therefore, the main generator terminal voltage is controlled indirectly.

This paper focuses on the control optimization algorithm for aircraft AC generator brushless excitation system, so the permanent magnet synchronous generator (auxiliary exciter) and its rectifier are replaced by DC power supply [13].

2.2. Main Synchronous Generator Model

The aircraft main generator of three-stage brushless AC excitation system is a wound rotor salient pole synchronous generator with damper windings. According to adopting the generator convention, the voltage equations of each phase windings of the stator, rotor and the flux linkage equations in ABC frame are acquired without considering the synchronous generator saturation, hysteresis and other factors. The model of main synchronous generator in dq0 frame is established as follows through the Park's transformation [14].

$$\begin{cases} u_{dm} = -R_s i_{dm} + L_q \omega_{em} i_{qm} - M_{sQ} \omega_{em} i_Q - L_d \dfrac{di_{dm}}{dt} \\ \qquad + M_{sf} \dfrac{di_f}{dt} + M_{sD} \dfrac{di_D}{dt} \\ u_{qm} = -R_s i_{qm} - L_d \omega_{em} i_{dm} + M_{sf} \omega_{em} i_f - L_q \dfrac{di_{qm}}{dt} \\ \qquad + M_{sD} \omega_{em} i_D + M_{sQ} \dfrac{di_Q}{dt} \\ v_f = R_f i_f - M_{sf} \dfrac{di_{dm}}{dt} + L_f \dfrac{di_f}{dt} + M_{fD} \dfrac{di_D}{dt} \\ 0 = R_D i_D - M_{sD} \dfrac{di_{dm}}{dt} + L_D \dfrac{di_D}{dt} + M_{fD} \dfrac{di_f}{dt} \\ 0 = R_Q i_Q - M_{sQ} \dfrac{di_{qm}}{dt} + L_Q \dfrac{di_Q}{dt} \end{cases} \quad (1)$$

Where, u, i, R, L, M are voltage, current, resistance, self-inductance, mutual inductance of the main generator in dq0 frame, respectively; The subscript symbol s denotes the main generator stator windings; dm, qm denote the direct and quadrature axis of stator windings, respectively; Subscript symbol f denotes the excitation windings; D, Q denote the direct and quadrature axis of the excitation windings, respectively.

2.3. Main Exciter Model

The main exciter is a salient pole synchronous generator that does not have two damper windings in d-q axis as compared to the main synchronous generator. According to adopting the generator convention, the model in dq0 frame of main exciter is established as follows:

$$\begin{cases} u_{de} = -R_{se} i_{de} + L_{qe} \omega_{ee} i_{qe} - L_{de} \dfrac{di_{de}}{dt} + M_{se} \dfrac{di_{ex}}{dt} \\ u_{qe} = -R_{se} i_{qe} - L_{de} \omega_{ee} i_{de} + M_{se} \omega_{ee} i_{ex} - L_{qe} \dfrac{di_{qe}}{dt} \\ u_{ex} = R_{ex} i_{ex} - M_{se} \dfrac{di_{de}}{dt} + L_{ex} \dfrac{di_{ex}}{dt} \end{cases} \quad (2)$$

Where, u , i , R , L , M denote voltage, current, resistance, self inductance, mutual inductance of the main exciter in dq0 frame, respectively; Subscript symbols se , ex denote the main exciter stator windings, excitation windings, respectively; de , qe denote the direct and quadrature axis of the stator windings, respectively.

3. DESIGN OF ADAPTIVE CONTTOLLER BASED ON MULTI-PARAMETER OPTIMIZATION

3.1. Improved Adaptive Particle Swarm Optimization Algorithm

Particle swarm optimization (PSO) is the stochastic optimization algorithm based on bionic swarm intelligence which was proposed by Kennedy and Eberhart in 1995. The solution space of the problem is analogous to a flock of birds foraging over certain areas, and each bird is modeled as a particle without mass or volume. Each particle represents a candidate solution to the problem with its own position and velocity. PSO can rapidly find the solution of the problem through the mutual cooperation among the bionic swarm intelligence particles. PSO is very suitable for solving nonlinear optimization problem in high-dimensional space, because it has an inherent parallel computational structure, and it does not require the derivative of the object function. PSO is preferred to other optimization algorithms for it has rapid convergence speed, easy implementation and fewer parameters to be adjusted.

In PSO, a swarm of particles are represented as potential solutions, and each particle i is associated with the velocity vector $V_i = [v_{i,1}, v_{i,2}, \cdots v_{i,d}]$ and the position vector $X_i = [x_{i,1}, x_{i,2}, \cdots x_{i,d}]$, where d denotes the dimension of the solution space. The velocity and the position of each particle are initialized by random vectors within the corresponding ranges. During the evolutionary process, the velocity and position of the i particle on jth dimension are updated as:

$$v_{i,j}(t+1) = \omega v_{i,j}(t) + c_1 r_1 [p_{i,j} - x_{i,j}(t)] + c_2 r_2 [p_{g,j} - x_{i,j}(t)] \quad (3)$$

$$x_{i,j}(t+1) = x_{i,j}(t) + v_{i,j}(t+1) \; j = 1,2,.....,d \quad (4)$$

Where, ω is the inertia weight; c_1 , c_2 denote positive acceleration coefficients, $r_1 r_2 \in [0,1]$ are random numbers; d denotes the dimension of the solution space; In order to prevent the optimal solution out of the optimization range, the general assumption is $v \in [v_{\min} \quad v_{\max}]$, $x \in [x_{\min} \quad x_{\max}]$.

The inertia weight (ω) of PSO is an important parameter that influences the convergence speed of PSO algorithm and decides the particle global search ability. Therefore, the proper selection of ω is crucial to the optimization quality of the PSO algorithm. The constant between [0.2, 1.2] or a linearly decreasing weight ω is adopted in many literatures.

$$\omega = \omega_{\max} - (\omega_{\max} - \omega_{\min}) \times g / G_{\max} \quad (5)$$

However, the PSO algorithm is used in a nonlinear dynamic process to search solution space in this paper. Therefore, the adaptive inertia weight is adopted, so that it is only related to current particle objective function value.

$$\omega = \begin{cases} \omega_{\min} + \dfrac{(\omega_{\max} - \omega_{\min})(J - J_{\min})}{J_{avg} - J_{\min}} & J \le J_{avg} \\ \omega_{\max} & J > J_{avg} \end{cases} \quad (6)$$

Where, $\omega_{\max}$ and $\omega_{\min}$ are the maximum and minimum inertia weight, respectively; J is the current particle objective function value; J_{avg} and $J_{\min}$ are average and minimum objective function values of all particles, respectively.

The adaptive weight is introduced into PSO algorithm, which can produce good global search ability, improve the effectiveness of rapid algorithm. Meanwhile, the optimal preservation strategy is adopted to ensure the algorithm converging quickly. During the process of optimizations, the worst individual in the current population is replaced by the best individual so far.

3.2. Design of RBFPID Controller Based on Multi-parameter Optimization

The Radial Basis Function (RBF) neural network is a kind of local approximation of the neural networks. It is more suitable for nonlinear real-time complex control system.

Considering the nonlinearity, strong coupling and time-varying characters of brushless excitation control system of aircraft AC generator, it is difficult for traditional Proportional Integral Derivative (PID) control to get good control performance. A compound excitation control strategy based on RBF and PID is designed in this section. To overcome the problem that the parameters of PID and RBF compound controller are difficult to be set, a new kind of multi-parameter adaptive optimization scheme is put forward based on adaptive particle swarm optimization (APSO) algorithm. The structure of RBFPID adaptive excitation controller is as shown in Fig. (**2**).

As you can see in Fig. (**2**), PID acts as a feedback controller which can suppress the interference and ensure the

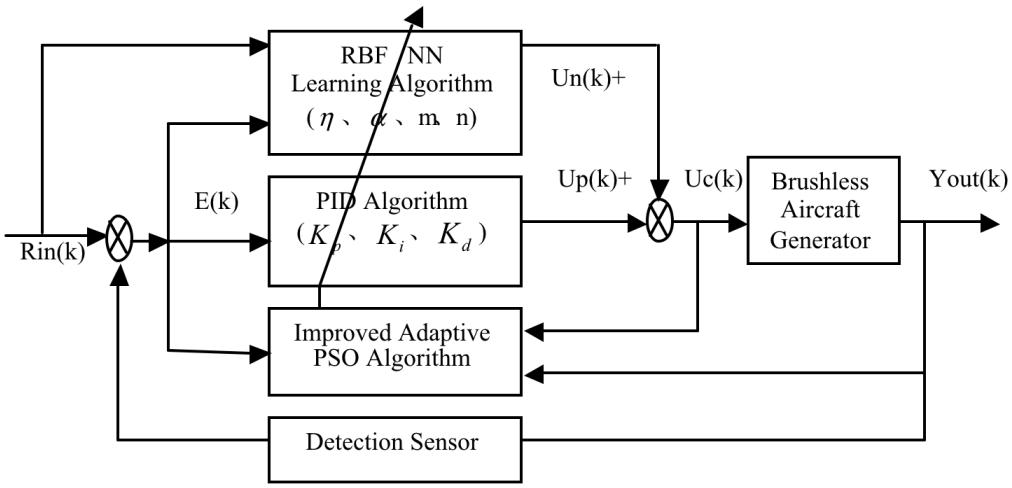

Fig. (2). PID and RBF adaptive controller based on PSO.

stability of the control system. RBF neural network is a feed-forward controller which can improve system response speed. The improved adaptive particle swarm algorithm is used to optimize multiple and mutual coupling control parameters of the compound RBFPID excitation controller, including learning rate (η), inertia weight (α), center vector (m), Gauss function width (n) of RBF neural network, and the proportional coefficient (Kp), integral coefficient (Ki), differential coefficient (Kd) of PID. Adaptive multi-parameter optimization enhances the control system dynamic stability, self-adaptive operation. The compound controller of RBFPID can adapt well to the change of control system conditions and uncertain factors, so as to improve the control quality of the excitation system.

In control stage, the adaptive excitation controller of RBFPID real-time detects the output voltage of main generator, and calculates and changes the control signal $U_c(k)$ (proportional to the duty ratio of PWM) according to the voltage error. The enlarged PWM signal controls the excitation current of main generator, and regulates generator output voltage. The control output of RBF neural network is expressed as follows.

$$h_j = \exp[-\frac{\left\|x(k)-c_j\right\|^2}{2\sigma_j^{\ 2}}] \qquad j=1,2,.....p \tag{7}$$

$$U_n(k)=\sum_{j=1}^{n}\omega_j h_j \qquad j=1,2,....p \tag{8}$$

Where, x is p dimension of input vector, $x \in R^n$. c_j is the *jth* central point of the radial basis function; σ_j is the first of neurons in the hidden layer radial basis function width;

The total output $U_c(k)$ of the compound controller is the sum of the RBF controller output $U_n(k)$ and PID controller output $U_p(k)$ which are optimized by APSO.

$$U_c(k)=U_n(k)+U_p(k) \tag{9}$$

At the end of each control cycle, the control system enters the learning stage, in which connect weights are adjusted according to the system error. The weights adjustment formula of RBF network is as follows:

$$E(k)=\frac{1}{2}(u_c(k)-u_n(k))^2 \tag{10}$$

$$\Delta\omega(k)=-\eta\frac{\partial E(k)}{\partial\omega_j(k)}=\eta(u_n(k)-u_c(k))h_j(k) \tag{11}$$

$$\omega(k)=\omega(k-1)+\Delta\omega(k)+\alpha(\omega(k)-\omega(k-1)) \tag{12}$$

Where η is the learning rate of RBF neural network, E(k) is tracking error of the control system, the purpose of learning minimizes the system error E(k).

3.3. Algorithm Implementation Steps

Assume P^t represents the t th generation of the population. $B\text{est}^t$ is the best individual among P^0, P^1, $\cdots$, P^t; $LB\text{est}^t$ is the best individual in P^t. The flow chart of multi-parameter optimization based on APSO is as shown in Fig. (**3**).

STEP 1: According to the general experience, the ranges [min, max] of seven optimized parameters are to be determined. Other parameters such as the number of maximum iteration G_{max}, population size N are to be set in the same time;

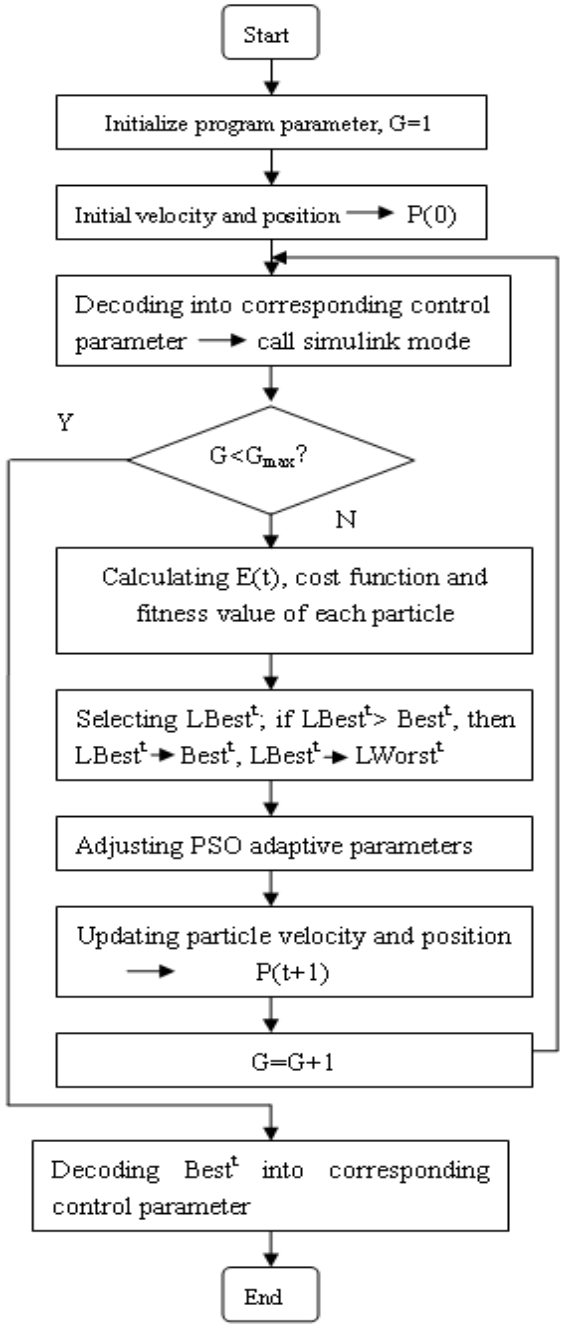

Fig. (3). Multi-parameter optimization based on APSO flow chart.

STEP 2: It randomly generates N individual particles to form the initial population P^0. Each of actual parameter is initialized as formula (13).

$$K = \min + (\max - \min) \times rand \tag{13}$$

Where, rand $\in (0,1)$ is a random number; the seven parameters form (K_p, K_i , K_d, η , α , m , n) individual;

STEP 3: Each individual is decoded into the corresponding control parameters. The result of system error $e(t)$ is obtained under the control of each set of decoded parameters;

STEP 4: According to the formula (14), the value J of the cost function is calculated for each individual, the fitness value is defined as 1/J. If $e(t) \le 0$, the cost function J is defined as the formula (15).

$$J = \int_0^\infty \left(w_1 \left| e(t) \right|^2 \right) dt \tag{14}$$

$$J = \int_0^\infty (w_1 \left| e(t) \right|^2 + w_2 \left| e(t) \right|) dt \tag{15}$$

Where, $e(t)$ is the system error; w_1, w_2 are the weights value, and, $e(t) = y(t) - y(t-1)$, $y(t)$ is the system output; the formula (15) is a penalty function which is used to avoid an overshoot;

STEP 5: According to the fitness value of each individual, the best and worst individuals are selected and saved to $LB\text{est}^t$ and $LW\text{orst}^t$, respectively;

STEP 6: $B\text{est}^t$ and $LB\text{est}^t$ are compared, if $LB\text{est}^t \rangle B\text{est}^t$, then $B\text{est}^t \leftarrow LB\text{est}^t$ and $LWorst^t \leftarrow B\text{est}^t$

STEP 7: Adjust the adaptive control parameters of PSO algorithm according to the formula (5) or formula (6);

STEP 8: Update particle velocity and position according to the formula (3) and formula (4), respectively and obtain P^{t+1};

STEP 9: Judging whether the iterations times reaches the preset value G_{max} or not. If so, end of program, else returns to step 3.

STEP 10: The best individual $B\text{est}^t$ after many generations of evolution is decoded as optimal control parameters.

4. SYSTEM SIMULATION ANALYSIS

According to the mathematical model of main exciter and main generator in section 2, the simplified excitation system simulation model of aircraft AC generator is established in SIMULINK as shown in Fig. (**4**) (upper part), in which the auxiliary exciter is replaced by DC voltage source.

The PID and RBF controller model based on APSO multi-parameter optimization for brushless excitation system of aircraft AC generators is shown in Fig. (**4**) (lower part). RBF and PID controllers are implemented through the two MATLAB functions, respectively. The system given voltage U_{ref} is 115V; U_{out} stands for the voltage effective value (RMS) of aircraft AC generator three-phase output voltage; The simulation parameters: $T_s = 1e-5s$, $n_N = 12000$ rpm, $U_{DC} = 60V$, $p = 2$. The ranges of adaptive parameters are

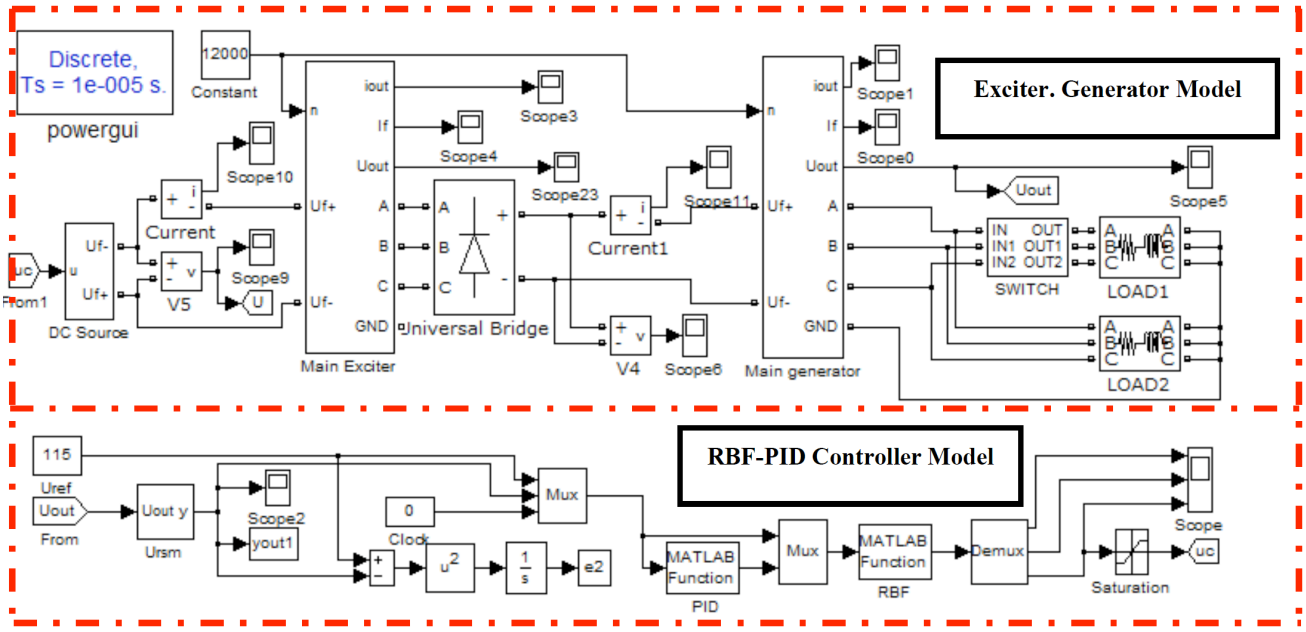

Fig. (4). Brushless excitation simulation control model for aircraft generator.

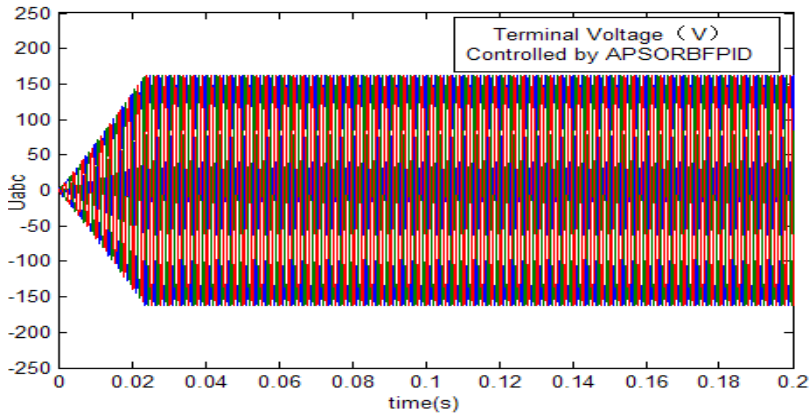

Fig. (5). Excitation simulation step response.

$m=[80 \quad 120]$, $n=[0 \quad 10]$, $Kp \in [50,650]$, $Ki \in [0,10]$, $Kd \in [0,30]$, $\eta \in [0.0,0.5]$, $\alpha \in [0.0,0.5]$, respectively.

4.1. Simulation of Raising Voltage From Zero

The simulation experiment of raising voltage from zero is used to validate reliability and rapidity of the proposed excitation control scheme for aircraft AC generator. The simulation time is 0.2s. Fig. (**5**) is the aircraft AC generator terminal voltage of raising voltage from zero simulation under the control of APSORBFPID., The simulation results under the adaptive PSOPID controller (APSOPID) is also given in Fig. (**6**) for comparison. Compared Fig. (**5**) with Fig. (**6**), it can be seen that the proposed APSORBFPID controller has the faster control speed than the APSOPID controller at the same experimental conditions.

The simulation RMS voltage curves of the raising voltage from zero experiment are shown in Fig. (**7**) (the red curve represents the terminal RMS voltage under the proposed algorithm of APSORBFPID, the green one is the terminal RMS voltage under the APSOPID controller, the dotted line is the given voltage 115V). As can be seen from the Fig. (**7**), the rise time of the PSOPIDRBF controller is shortened obviously, only 21.5ms. Meanwhile the rise time of the PSOPID controller is 31.8ms. The control accuracy of the former is higher than that of the latter.

The control parameters and control performance of two excitation controllers are given in Table **1**. From the Table **1**, it can be seen that the terminal voltage error of aircraft AC generator is only 0.0035V under the control of APSORBFPID, and it is far less the error 0.0815V under the control of APSOPID. It also can be seen from the Table **1**, the overshoot of the system voltage is only 0.17% under the control of APSORBFPID. Comparative analysis indicates that the GAPIDRBF controller achieves better performance.

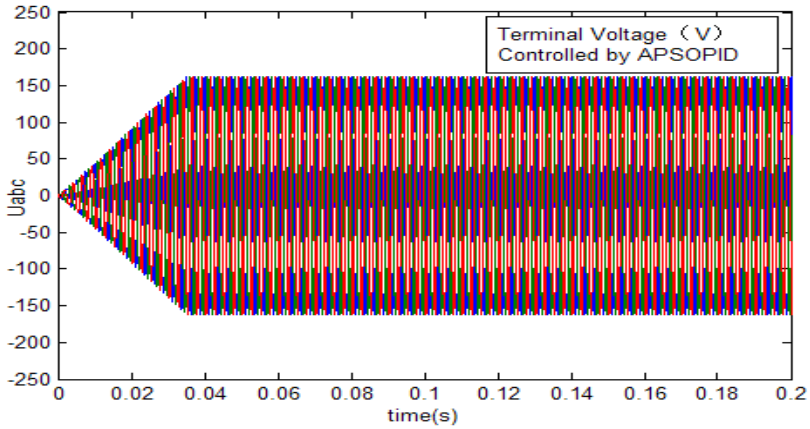

Fig. (6). Excitation simulation step response.

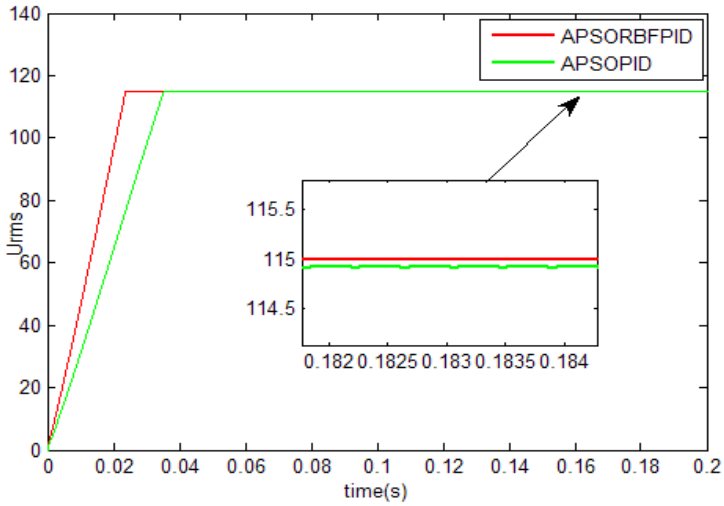

Fig. (7). Excitation simulation step response.

Table 1. Comparison of the step response results of two excitation controllers.

Control Parameters and Performance Parameters											
Controller	**Kp**	**Ki**	**Kd**	η	α	**m**	**n**	**J**	**E (V)**	**M%**	**Tr/ms**
APSOPID	371.2897	0.10	0.100	/	/	/	/	160.6700	0.0815	0.00	31.8
APSORBFPID	634.9522	0.0	0.100	0. 3000	0.020	114.9522	1.000	109.8333	0.0035	0.17	21.5

4.2. Simulation of Plus/Minus Load

In order to validate anti-interference capability of the proposed excitation control scheme, the 20% rated load is suddenly connected to the system model at the time 0.25s. At the time 0.35s, the 20% rated load is suddenly disconnected to the system model. The AC voltage curves are given in Fig. (**8**), Fig. (**9**) under the control of PID controller and APSORBFPID controller, respectively.

In Fig. (**8**), when 20% rated load is suddenly added at time 0.25s, the terminal AC voltage experiences an obvious decrease. While 20% load is shaded at the time 0.35s, the terminal AC voltage increases quickly. Comparing with Fig. (**8**), From Fig. (**9**), it can be seen that the terminal AC voltage change is very small under the control of APSORBFPID, whether 20% rated load is suddenly connected at the time 0.25s, or disconnected at the time 0.35s.

The RMS voltage curves are given in Fig. (**10**) under the control of two controllers. From Fig. (**10**), the proposed APSORBFPID control scheme not only has more rapid the response speed and also has higher control precision. The terminal voltage error under the APSORBFPID control is smaller than that of APSOPID.

The output control signals of APSORBFPID and APSOPID controllers are given in Fig. (**11**). From Fig. (**11**), the

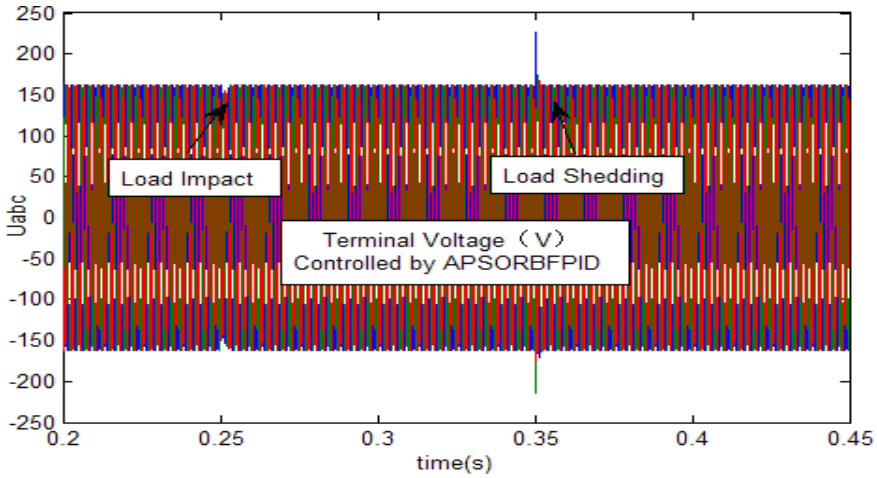

Fig. (8). Output control signal under the model uncertain.

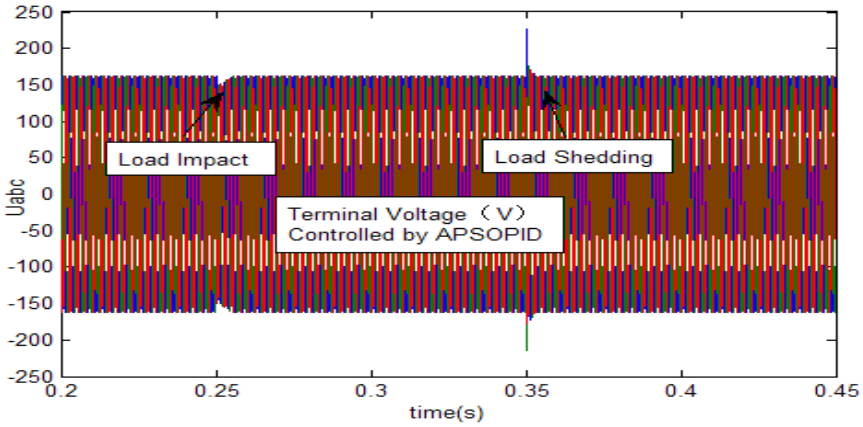

Fig. (9). Output control signal under the model uncertain.

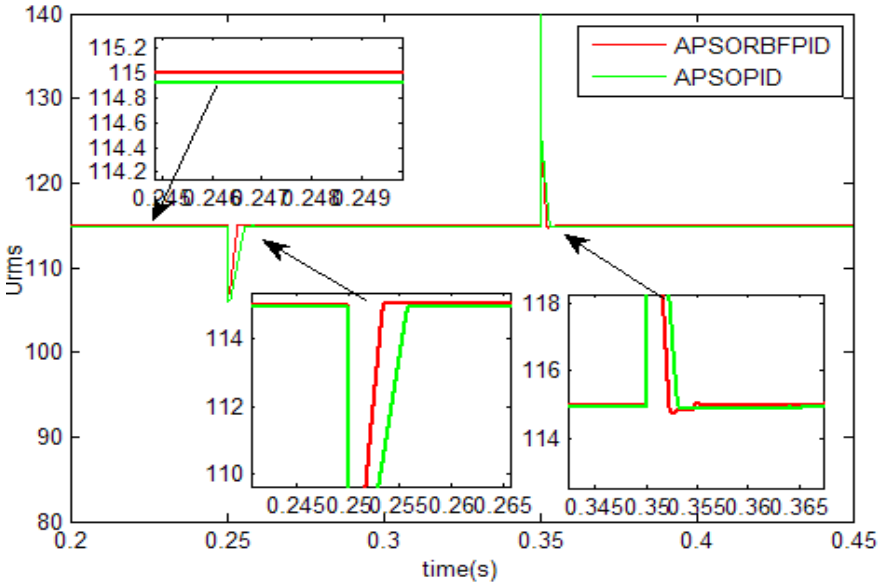

Fig. (10). Output control signal under the model uncertain.

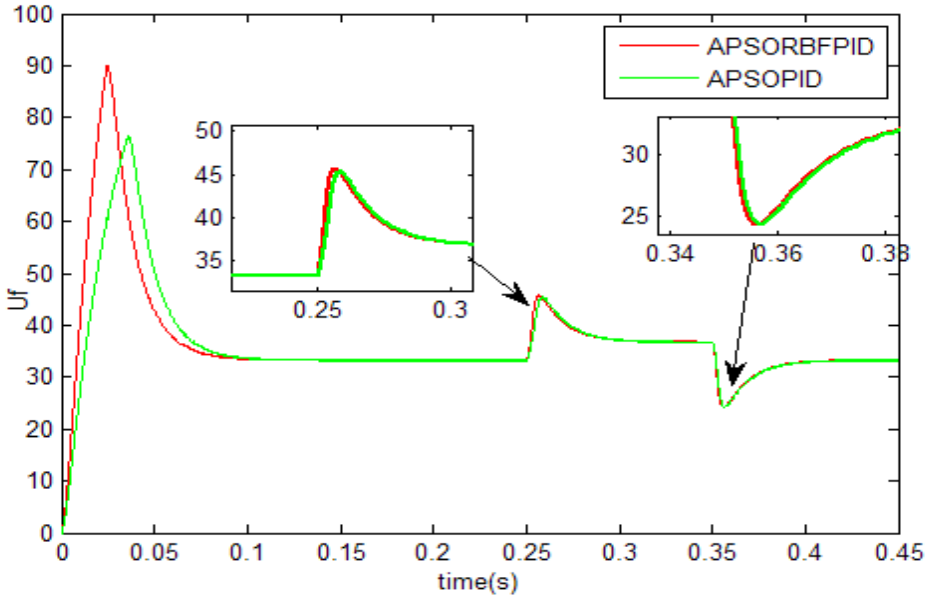

Fig. (11). Output voltages under the model uncertain.

control signal output of APSORBFPID controller is always more quickly tracking any change of the system load than that of APSOPID controller.

CONCLUSION

This paper presents an effective multi-parameter optimization scheme to design a new RBF and PID excitation controller (APSORBFPID) for three-stage aircraft AC generator based on adaptive particle swarm optimization (APSO). The new control strategy combines all advantages of adaptive particle swarm optimization, RBF neural network and PID controller. The simulation results show the proposed compound APSORBFPID excitation controller for aircraft AC generator has smaller voltage error, shorter adjusting time, and faster response than the conventional PID excitation controller. Meanwhile, the novel multi-parameter optimization based on APSO overcomes the problem that multiple parameters are difficult to tune because of mutual coupling in conventional compound controller.

CONFLICT OF INTEREST

The authors confirm that this article content has no conflict of interest.

ACKNOWLEDGEMENTS

This work was supported by the National Natural Science Foundation of China under Grant No.51167013 and No.51567019, Natural Science Foundation of Jiangxi Province under Grant No. 20122BAB201019, S&T Pillar Project of Jiangxi Province under 20142BBE50002.

REFERENCES

[1] L. Cheng, J. Zhang, Y. Sun, X. Guan, C. Wu, and W. Li,"Closed-loop optimum design method for PID controller of excitation system in large-scale power system", *Power System Technology*, vol. 31, no. 3, pp. 49-53, 2007.

[2] A.P. Memon, M.A. Uqaili, Z.A. Memon and N.K. Tanwani, "Suitable feed forward artificial neural network automatic voltage regulator for excitation control system", *Universal Journal of Electrical and Electronic Engineering*, vol. 2, no. 2, pp. 45-51, 2014.

[3] H. Jie, J. Kang, and P. Li, "Fuzzy PID controller based on variable universe for excitation system", *Electric Power Automation Equipment*, vol. 38, no. 2, pp. 101-104, 2011.

[4] L. Sun, H. Song, C. Gong and K. Ma, "Disturbance signal for parameter identification of excitation system and accuracy analysis", *Water Resources and Power*, vol. 31, no. 6, pp. 177-181, 2013.

[5] J. Zhao, and J. Chen, "Design of the fuzzy neural PID controller based on hybrid PSO", *Journal of Xidian University*, vol. 35, no. 1, pp. 54-59, 2008.

[6] L. Zhang, and Y. Bo, "PID adaptive control in the application of the induction motor system based on the RBF neural network inverse", *Journal of Applied Mechanics and Materials Research*, vol. 556-562, no. 2014, pp. 2393-2396.

[7] J. Zhang, G. Wen, Y. Wei, and G. Yin, "RBF neural network pid for bilateral servo control system", *Journal of TELKOMNIKA*, vol. 11, no. 9, pp. 5200-5209, 2013.

[8] W. Nie, and Z. Wang, "Design of direct torque control system of motor based on RBF neural network supervision", *Journal of Industry and Mine Automation*, vol. 39, no. 10, pp. 52-55, 2013.

[9] H. Fang, and Z. Shen, "Optimal hydraulic turbogenerators PID governor tuning with an improved particle swarm optimization algorithm", *Proceedings of the CSEE*, vol. 25, no. 22, pp. 120-124, 2005.

[10] J. Liu, *Advanced PID Control and MATLAB Simulation*, Electronic Industry Press, Beijing, 2003.

[11] X. Zhang, and Y. Wang, "Research on improved on-line learning algorithm of RBF neural network", *Journal of Changzhou University (Natural Science Edition)*, vol. 26, no. 1, pp. 52-56, 2014.

[12] M. Gunes and N. Dogru, "Fuzzy control of brushless excitation system for steam turbogenerators", *IEEE Transactions On Energy Conversion*, vol. 25, no. 3, pp. 844-852, 2010.

[13] B. Liang, Y. Li, and M. Xue, "Modeling and simulation of three-stage aircraft synchronous generator system", *Journal of Computer Simulation*, vol. 30, no. 10, pp. 71-75, 2013.

[14] A. Barakat, S. lim Tnani, G. Champenois, and E. Mouni. A new approach for synchronous generator terminal voltage control - Comparison with a standard industrial controller. *Electric Power Systems Researc*h, vol. 81, no. 7, pp. 1592-1601, 2011.

Received: September 16, 2014 Revised: December 23, 2014 Accepted: December 31, 2014